Graham Garland Ross

13 September 1944 — 31 October 2021

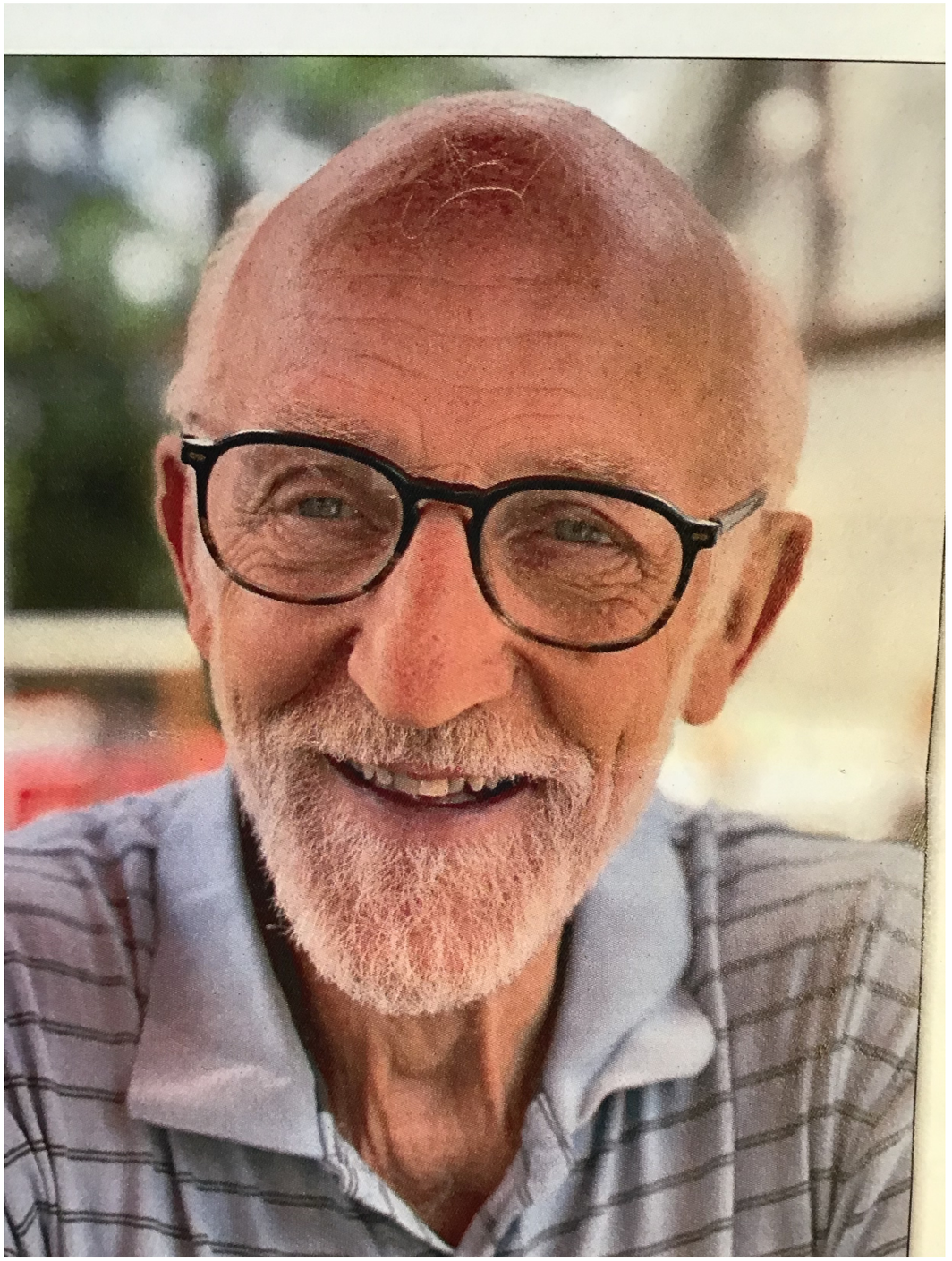

Graham has worked on:
gauge theories, supersymmetry, fermion masses, in particular neutrino masses, many aspects of BSM physics, inflationary cosmology . . .

Graham has worked on:
gauge theories, supersymmetry, fermion masses, in particular neutrino masses, many aspects of BSM physics, inflationary cosmology . . .

. . . string phenomenology:

Graham has worked on:
gauge theories, supersymmetry, fermion masses, in particular neutrino masses, many aspects of BSM physics, inflationary cosmology . . .

. . . string phenomenology:

Volume 180, number 1,2 PHYSICS LETTERS B 6 November 1986

A SUPERSTRING-INSPIRED STANDARD MODEL

Brian R. GREENE [1], Kelley H. KIRKLIN [1], Paul J. MIRON and Graham G. ROSS

Department of Theoretical Physics, University of Oxford, 1 Keble Road, Oxford OX1 3RH, UK

Received 3 June 1986; revised manuscript received 12 August 1986

An analysis is presented of an $E_8 \otimes E_8$ superstring-inspired ten-dimensional supergravity model following from compactification on a particular Calabi–Yau manifold which gives rise to three generations. The multiplet structure and discrete symmetries after compactification are determined. It is shown that the model has flat directions which allow for breaking of the gauge group to the standard $SU(3) \otimes SU(2) \otimes U(1)$ model at a high scale. The resulting low-energy theory has a realistic spectrum and, remarkably, the discrete symmetries predict a reasonable structure for the Kobayashi–Maskawa mixing matrix. Without unnatural adjustments, proton decay is inhibited and neutrino masses consistent with experimental limits are obtained.

A short conversation (~ 10 mins) with Graham would easily cover:

A short conversation (~ 10 mins) with Graham would easily cover:

- How his family is doing.

A short conversation (~ 10 mins) with Graham would easily cover:

- How his family is doing.

- How your family is doing.

A short conversation (~ 10 mins) with Graham would easily cover:

- How his family is doing.
- How your family is doing.
- Modular functions and fermion mass models in string theory.

A short conversation (~ 10 mins) with Graham would easily cover:

- How his family is doing.
- How your family is doing.
- Modular functions and fermion mass models in string theory.
- Scale invariance as an attempt to address the hierarchy problem.

A short conversation (~ 10 mins) with Graham would easily cover:

- How his family is doing.
- How your family is doing.
- Modular functions and fermion mass models in string theory.
- Scale invariance as an attempt to address the hierarchy problem.
- How f***ed up the UK is.

A short conversation (~ 10 mins) with Graham would easily cover:

- How his family is doing.
- How your family is doing.
- Modular functions and fermion mass models in string theory.
- Scale invariance as an attempt to address the hierarchy problem.
- How f***ed up the UK is.
- Models of inflation.

A short conversation (~ 10 mins) with Graham would easily cover:

- How his family is doing.
- How your family is doing.
- Modular functions and fermion mass models in string theory.
- Scale invariance as an attempt to address the hierarchy problem.
- How f***ed up the UK is.
- Models of inflation.
- Scottish independence


50
20
10
80
90
100
110
120
Higgs Mass /GeV
Focus point

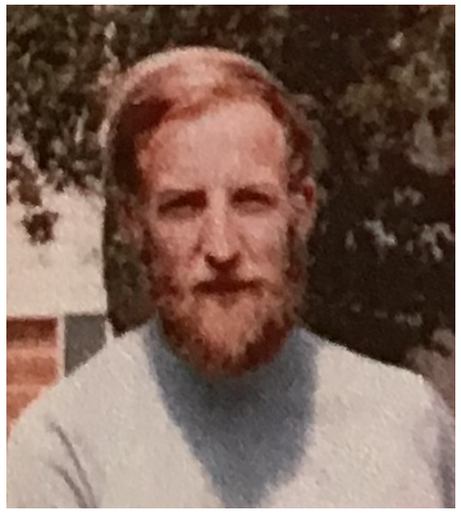

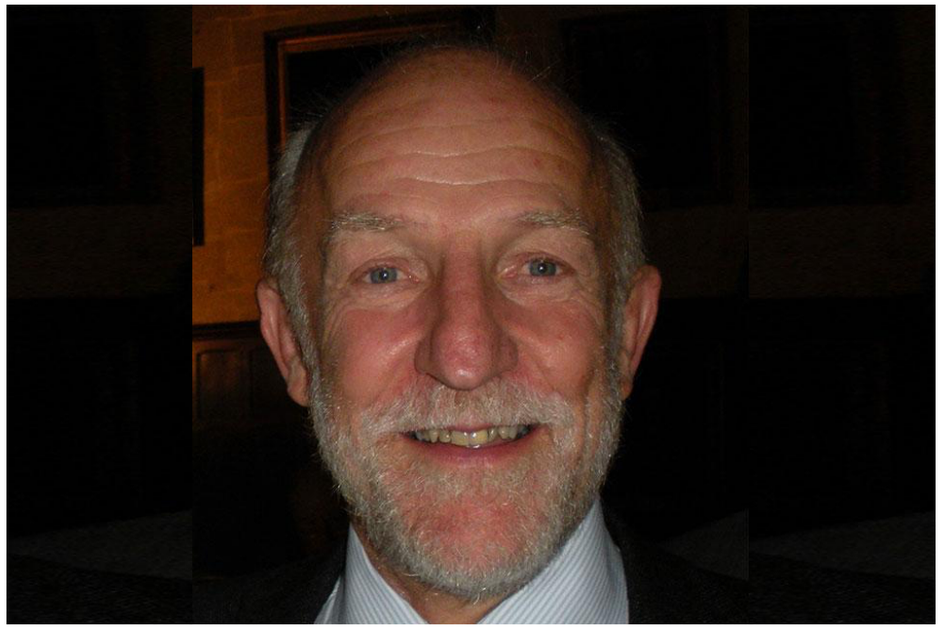

Numerical Calabi-Yau Metrics from Machine Learning

Andre Lukas
University of Oxford

String Pheno 2022, Liverpool, July 2022

based on 2211.010436, 2205.13408

In collaboration with: Magdalena Larfors, Fabian Ruehle, Robin Schneider

Outline

- Introduction
- Mathematical background
- Computational realisation
- Results
- Conclusion

Introduction

Analytic expressions for Ricci-flat metrics on (compact) CY n-folds are not known, for n>2. (K3 case, see: Kachru, Tripathy, Zimet, 1810.10540, 2006.2436,

Introduction

Analytic expressions for Ricci-flat metrics on (compact) CY n-folds are not known, for n>2. (K3 case, see: Kachru, Tripathy, Zimet, 1810.10540, 2006.2436,

For CY compactifications the massless spectrum and holomorphic low-energy quantities (superpotential) do not depend on Ricci-flat metric.

Introduction

Analytic expressions for Ricci-flat metrics on (compact) CY n-folds are not known, for n>2. (K3 case, see: Kachru, Tripathy, Zimet, 1810.10540, 2006.2436,

For CY compactifications the massless spectrum and holomorphic low-energy quantities (superpotential) do not depend on Ricci-flat metric.

However, the massive spectrum and non-holomorphic quantities (matter field Kahler metric, physical Yukawa couplings) do depend on Ricci-flat metric.

Introduction

Analytic expressions for Ricci-flat metrics on (compact) CY n-folds are not known, for n>2. (K3 case, see: Kachru, Tripathy, Zimet, 1810.10540, 2006.2436,

For CY compactifications the massless spectrum and holomorphic low-energy quantities (superpotential) do not depend on Ricci-flat metric.

However, the massive spectrum and non-holomorphic quantities (matter field Kahler metric, physical Yukawa couplings) do depend on Ricci-flat metric.

-> Computing fermion masses from string theory requires the Ricci-flat CY metric.

Introduction

Analytic expressions for Ricci-flat metrics on (compact) CY n-folds are not known, for n>2. (K3 case, see: Kachru, Tripathy, Zimet, 1810.10540, 2006.2436,

For CY compactifications the massless spectrum and holomorphic low-energy quantities (superpotential) do not depend on Ricci-flat metric.

However, the massive spectrum and non-holomorphic quantities (matter field Kahler metric, physical Yukawa couplings) do depend on Ricci-flat metric.

-> Computing fermion masses from string theory requires the Ricci-flat CY metric.

-> Compute Ricci-flat CY metric numerically.

Numerical CY metrics and ML:

Ashmore, He, Ovrut, 1910.08605, Donaldson algorithms + ML

Ashmore, Ruehle, 2103.07472, ML, CY metrics and swampland distance conj.

Douglas, Lakshminarasimhan, Qi, 2012.04797, holomorphic networks

Jejjala, Mayorga Pena, Mishra, 2012.15821, quintic and Tian-Yau

Anderson, Gerdes, Gray, Krippendorf, Raghuram, Ruehle, 2012.04797,
moduli dependence, SU(3) structure

Ashmore, Deen, He, Ovrut, 2110.12483, line bundle connections on CYs

Ashmore, Calmon, He, Ovrut, 2112.10872, ML and energy functionals

Larfors, Lukas, Ruehle, Schneider, 2211.010436, 2205.13408, all CICYs and KS CYs

. . .

Numerical CY metrics and ML:

Ashmore, He, Ovrut, 1910.08605, Donaldson algorithms + ML

Ashmore, Ruehle, 2103.07472, ML, CY metrics and swampland distance conj.

Douglas, Lakshminarasimhan, Qi, 2012.04797, holomorphic networks

Jejjala, Mayorga Pena, Mishra, 2012.15821, quintic and Tian-Yau

Anderson, Gerdes, Gray, Krippendorf, Raghuram, Ruehle, 2012.04797,
moduli dependence, SU(3) structure

Ashmore, Deen, He, Ovrut, 2110.12483, line bundle connections on CYs

Ashmore, Calmon, He, Ovrut, 2112.10872, ML and energy functionals

Larfors, Lukas, Ruehle, Schneider, 2211.010436, 2205.13408, all CICYs and KS CYs

. . .

this talk

Numerical CY metrics and ML:

Ashmore, He, Ovrut, 1910.08605, Donaldson algorithms + ML

Ashmore, Ruehle, 2103.07472, ML, CY metrics and swampland distance conj.

Douglas, Lakshminarasimhan, Qi, 2012.04797, holomorphic networks

Jejjala, Mayorga Pena, Mishra, 2012.15821, quintic and Tian-Yau

Anderson, Gerdes, Gray, Krippendorf, Raghuram, Ruehle, 2012.04797,
moduli dependence, SU(3) structure

Ashmore, Deen, He, Ovrut, 2110.12483, line bundle connections on CYs

Ashmore, Calmon, He, Ovrut, 2112.10872, ML and energy functionals

Larfors, Lukas, Ruehle, Schneider, 2211.010436, 2205.13408, all CICYs and KS CYs

. . .

this talk

Key points:

- Compute Ricci-flat metric for CICYs and KS CYs.
- Compute Ricci-flat metric at given point in moduli space.
- Realised in python/tensorflow library with Mathematica api:

https://github.com/pythoncymetric/cymetric

Mathematical background

Yau's theorem

For a CY manifold X with Kahler form J' there exists a unique Kahler form J_{CY} with $[J_{\mathrm{CY}}] = [J']$ and an associated Ricci-flat metric $g_{\mathrm{CY},a\bar{b}} = -iJ_{\mathrm{CY},a\bar{b}}$.

Mathematical background

Yau's theorem

For a CY manifold X with Kahler form J' there exists a unique Kahler form $J_{\rm CY}$ with $[J_{\rm CY}] = [J']$ and an associated Ricci-flat metric $g_{{\rm CY},a\bar{b}} = -iJ_{{\rm CY},a\bar{b}}$.

Monge-Ampere equation

$J_{\rm CY}$ can be found by solving

$$J_{\rm CY} \wedge J_{\rm CY} \wedge J_{\rm CY} = \kappa\, \Omega \wedge \bar{\Omega} \qquad \text{with} \qquad J_{\rm CY} = J' + \partial\bar{\partial}\phi$$

Mathematical background

Yau's theorem

For a CY manifold X with Kahler form J' there exists a unique Kahler form $J_{\rm CY}$ with $[J_{\rm CY}] = [J']$ and an associated Ricci-flat metric $g_{{\rm CY},a\bar{b}} = -iJ_{{\rm CY},a\bar{b}}$.

Monge-Ampere equation

$J_{\rm CY}$ can be found by solving

$$J_{\rm CY} \wedge J_{\rm CY} \wedge J_{\rm CY} = \kappa\, \Omega \wedge \bar{\Omega} \qquad \text{with} \qquad J_{\rm CY} = J' + \partial\bar{\partial}\phi$$

CY manifolds

We consider CYs $X \subset \mathcal{A}$ in an ambient space $\mathcal{A}$ of two types:

Mathematical background

Yau's theorem

For a CY manifold X with Kahler form J' there exists a unique Kahler form $J_{\rm CY}$ with $[J_{\rm CY}] = [J']$ and an associated Ricci-flat metric $g_{{\rm CY},a\bar{b}} = -iJ_{{\rm CY},a\bar{b}}$.

Monge-Ampere equation

$J_{\rm CY}$ can be found by solving

$$J_{\rm CY} \wedge J_{\rm CY} \wedge J_{\rm CY} = \kappa\, \Omega \wedge \bar{\Omega} \qquad \text{with} \qquad J_{\rm CY} = J' + \partial\bar{\partial}\phi$$

CY manifolds

We consider CYs $X \subset \mathcal{A}$ in an ambient space $\mathcal{A}$ of two types:

$$X = \text{complete intersection} \quad \subset \quad \mathcal{A} = \mathbb{P}^{n_1} \times \cdots \times \mathbb{P}^{n_m} \quad \text{(CICYs)}$$

$$X = \text{hypersurface} \quad \subset \quad \mathcal{A} = \text{toric 4-fold} \quad \text{(Kreuzer-Skarke CY)}$$

Mathematical background

Yau's theorem

For a CY manifold X with Kahler form J' there exists a unique Kahler form $J_{\rm CY}$ with $[J_{\rm CY}] = [J']$ and an associated Ricci-flat metric $g_{{\rm CY},a\bar{b}} = -iJ_{{\rm CY},a\bar{b}}$.

Monge-Ampere equation

$J_{\rm CY}$ can be found by solving

$$J_{\rm CY} \wedge J_{\rm CY} \wedge J_{\rm CY} = \kappa\, \Omega \wedge \bar{\Omega} \qquad \text{with} \qquad J_{\rm CY} = J' + \partial\bar{\partial}\phi$$

CY manifolds

We consider CYs $X \subset \mathcal{A}$ in an ambient space $\mathcal{A}$ of two types:

$$X = \text{complete intersection} \quad \subset \quad \mathcal{A} = \mathbb{P}^{n_1} \times \cdots \times \mathbb{P}^{n_m} \quad \text{(CICYs)}$$

$$X = \text{hypersurface} \quad \subset \quad \mathcal{A} = \text{toric 4-fold} \quad \text{(Kreuzer-Skarke CY)}$$

$$J' = J_{\rm FS} = t^\alpha J_\alpha$$

Mathematical background

Yau's theorem

For a CY manifold X with Kahler form J' there exists a unique Kahler form $J_{\rm CY}$ with $[J_{\rm CY}] = [J']$ and an associated Ricci-flat metric $g_{{\rm CY},a\bar{b}} = -iJ_{{\rm CY},a\bar{b}}$.

Monge-Ampere equation

$J_{\rm CY}$ can be found by solving

$$J_{\rm CY} \wedge J_{\rm CY} \wedge J_{\rm CY} = \kappa\, \Omega \wedge \bar{\Omega} \qquad \text{with} \qquad J_{\rm CY} = J' + \partial\bar{\partial}\phi$$

CY manifolds

We consider CYs $X \subset \mathcal{A}$ in an ambient space $\mathcal{A}$ of two types:

$$X = \text{complete intersection} \quad \subset \quad \mathcal{A} = \mathbb{P}^{n_1} \times \cdots \times \mathbb{P}^{n_m} \quad \text{(CICYs)}$$

$$X = \text{hypersurface} \quad \subset \quad \mathcal{A} = \text{toric 4-fold} \quad \text{(Kreuzer-Skarke CY)}$$

$$J' = J_{\rm FS} = t^\alpha J_\alpha \longleftarrow \text{by restriction from } \mathcal{A}$$

t^α: Kahler moduli

Volume forms and integration

$$\mathrm{dVol}_{\mathrm{FS}} = \frac{1}{3!} J_{\mathrm{FS}}^3 \qquad \mathrm{dVol}_{\mathrm{CY}} = \frac{1}{3!} J_{\mathrm{CY}}^3 = \frac{\kappa}{3!} \mathrm{dVol}_{\Omega} \qquad \mathrm{dVol}_{\Omega} = \Omega \wedge \bar{\Omega}$$

Volume forms and integration

$$\mathrm{dVol}_{\mathrm{FS}} = \frac{1}{3!} J_{\mathrm{FS}}^3 \qquad \mathrm{dVol}_{\mathrm{CY}} = \frac{1}{3!} J_{\mathrm{CY}}^3 = \frac{\kappa}{3!} \mathrm{dVol}_{\Omega} \qquad \mathrm{dVol}_{\Omega} = \Omega \wedge \bar{\Omega}$$

typical problem: integrate function $f : X \to \mathbb{C}$ over CY

$$\int_X \mathrm{dVol}_{\mathrm{CY}}\, f = \int_X d^6 y \sqrt{g_{\mathrm{CY}}}\, f \;, \qquad \int_X \mathrm{dVol}_{\mathrm{FS}}\, f = \int_X d^6 y \sqrt{g_{\mathrm{FS}}}\, f$$

Volume forms and integration

$$\mathrm{dVol}_{\mathrm{FS}} = \frac{1}{3!} J_{\mathrm{FS}}^3 \qquad \mathrm{dVol}_{\mathrm{CY}} = \frac{1}{3!} J_{\mathrm{CY}}^3 = \frac{\kappa}{3!} \mathrm{dVol}_\Omega \qquad \mathrm{dVol}_\Omega = \Omega \wedge \bar{\Omega}$$

typical problem: integrate function $f : X \to \mathbb{C}$ over CY

$$\int_X \mathrm{dVol}_{\mathrm{CY}}\, f = \int_X d^6 y \sqrt{g_{\mathrm{CY}}}\, f\ , \qquad \int_X \mathrm{dVol}_{\mathrm{FS}}\, f = \int_X d^6 y \sqrt{g_{\mathrm{FS}}}\, f$$

CY volume: $\mathrm{Vol}_t(X) = \int_X \mathrm{dVol}_{\mathrm{CY}} = \int_X \mathrm{dVol}_{\mathrm{FS}} = \frac{1}{3!} d_{\alpha\beta\gamma} t^\alpha t^\beta t^\gamma$

Volume forms and integration

$$\mathrm{dVol}_{\mathrm{FS}} = \frac{1}{3!} J_{\mathrm{FS}}^3 \qquad \mathrm{dVol}_{\mathrm{CY}} = \frac{1}{3!} J_{\mathrm{CY}}^3 = \frac{\kappa}{3!} \mathrm{dVol}_\Omega \qquad \mathrm{dVol}_\Omega = \Omega \wedge \bar{\Omega}$$

typical problem: integrate function $f : X \to \mathbb{C}$ over CY

$$\int_X \mathrm{dVol}_{\mathrm{CY}}\, f = \int_X d^6 y \sqrt{g_{\mathrm{CY}}}\, f\ , \qquad \int_X \mathrm{dVol}_{\mathrm{FS}}\, f = \int_X d^6 y \sqrt{g_{\mathrm{FS}}}\, f$$

CY volume: $\mathrm{Vol}_t(X) = \int_X \mathrm{dVol}_{\mathrm{CY}} = \int_X \mathrm{dVol}_{\mathrm{FS}} = \frac{1}{3!} d_{\alpha\beta\gamma} t^\alpha t^\beta t^\gamma$

Line bundle slopes

Line bundle $\mathcal{O}_X(k)$ with curvature $F_{\mathrm{FS}} = 2\pi i k^\alpha J_\alpha$ and slope

$$\mu_t(\mathcal{O}_X(k)) = \int_X J_{\mathrm{CY}}^2 \wedge c_1(\mathcal{O}_X(k)) = \int_X J_{\mathrm{FS}}^2 \wedge c_1(\mathcal{O}_X(k)) = d_{\alpha\beta\gamma}\, t^\alpha t^\beta k^\gamma$$

Volume forms and integration

$$\mathrm{dVol}_{\mathrm{FS}} = \frac{1}{3!} J_{\mathrm{FS}}^3 \qquad \mathrm{dVol}_{\mathrm{CY}} = \frac{1}{3!} J_{\mathrm{CY}}^3 = \frac{\kappa}{3!} \mathrm{dVol}_{\Omega} \qquad \mathrm{dVol}_{\Omega} = \Omega \wedge \bar{\Omega}$$

typical problem: integrate function $f : X \to \mathbb{C}$ over CY

$$\int_X \mathrm{dVol}_{\mathrm{CY}}\, f = \int_X d^6 y \sqrt{g_{\mathrm{CY}}}\, f\ , \qquad \int_X \mathrm{dVol}_{\mathrm{FS}}\, f = \int_X d^6 y \sqrt{g_{\mathrm{FS}}}\, f$$

CY volume: $\mathrm{Vol}_t(X) = \int_X \mathrm{dVol}_{\mathrm{CY}} = \int_X \mathrm{dVol}_{\mathrm{FS}} = \frac{1}{3!} d_{\alpha\beta\gamma} t^\alpha t^\beta t^\gamma$

Line bundle slopes

Line bundle $\mathcal{O}_X(k)$ with curvature $F_{\mathrm{FS}} = 2\pi i k^\alpha J_\alpha$ and slope

$$\mu_t(\mathcal{O}_X(k)) = \int_X J_{\mathrm{CY}}^2 \wedge c_1(\mathcal{O}_X(k)) = \int_X J_{\mathrm{FS}}^2 \wedge c_1(\mathcal{O}_X(k)) = d_{\alpha\beta\gamma}\, t^\alpha t^\beta k^\gamma$$

$$\Longrightarrow \quad \mu_t(\mathcal{O}_X(k)) = \frac{2}{\pi} \int_X \mathrm{dVol}_{\mathrm{CY}}\, \rho_{\mathrm{CY}} = \frac{2}{\pi} \int_X \mathrm{dVol}_{\mathrm{FS}}\, \rho_{\mathrm{FS}} \qquad \text{where} \qquad \rho_{\mathrm{FS}} = \frac{1}{2} g_{\mathrm{FS}}^{a\bar{b}} F_{\mathrm{FS},a\bar{b}}\ , \quad \rho_{\mathrm{CY}} = \frac{1}{2} g_{\mathrm{CY}}^{a\bar{b}} F_{\mathrm{FS},a\bar{b}}$$

Numerical integration

Point sample $p_i \in X$ distributed according to known measure dA :

$$\int_X \mathrm{dVol}_{\mathrm{CY}}\, f \simeq \frac{1}{N}\sum_{i=1}^{N} \tilde{w}_i \det(g_{\mathrm{CY}}(p_i))\, f(p_i)\ , \qquad \tilde{w}_i = \left.\frac{d^6y}{dA}\right|_{p_i}$$

Numerical integration

Point sample $p_i \in X$ distributed according to known measure dA :

$$\int_X \mathrm{dVol}_{\mathrm{CY}}\, f \simeq \frac{1}{N}\sum_{i=1}^{N} \tilde{w}_i \det(g_{\mathrm{CY}}(p_i))\, f(p_i)\ , \qquad \tilde{w}_i = \left.\frac{d^6y}{dA}\right|_{p_i}$$

weights

Numerical integration

Point sample $p_i \in X$ distributed according to known measure dA :

$$\int_X \mathrm{dVol}_{\mathrm{CY}}\, f \simeq \frac{1}{N}\sum_{i=1}^{N} \tilde{w}_i \det(g_{\mathrm{CY}}(p_i))\, f(p_i)\,, \qquad \tilde{w}_i = \left.\frac{d^6y}{dA}\right|_{p_i}$$

weights

-> two tasks: 1) Generate point sample and 2) compute metric

Numerical integration

Point sample $p_i \in X$ distributed according to known measure dA :

$$\int_X \mathrm{dVol}_{\mathrm{CY}}\, f \simeq \frac{1}{N}\sum_{i=1}^{N} \tilde{w}_i \det(g_{\mathrm{CY}}(p_i))\, f(p_i)\,, \qquad \tilde{w}_i = \left.\frac{d^6y}{dA}\right|_{p_i}$$

weights

-> two tasks: 1) Generate point sample and 2) compute metric

Point sampling

CICYs: Use a thm by Shiffman and Zelditch which leads to point sample distributed according to a measure dA based on Fubini-Study forms.

Shiffman, Zelditch, CMP 200 (1999) 661.

Douglas, Karp, Lucik, Reinbacher, hep-th/0612075

Braun, Brelidze, Douglas, Ovrut, 0712.3563

Numerical integration

Point sample $p_i \in X$ distributed according to known measure dA :

$$\int_X \mathrm{dVol}_{\mathrm{CY}}\, f \simeq \frac{1}{N}\sum_{i=1}^{N} \tilde{w}_i \det(g_{\mathrm{CY}}(p_i))\, f(p_i)\,, \qquad \tilde{w}_i = \left.\frac{d^6y}{dA}\right|_{p_i}$$

weights

-> two tasks: 1) Generate point sample and 2) compute metric

Point sampling

CICYs: Use a thm by Shiffman and Zelditch which leads to point sample distributed according to a measure dA based on Fubini-Study forms.

Shiffman, Zelditch, CMP 200 (1999) 661.
Douglas, Karp, Lucik, Reinbacher, hep-th/0612075
Braun, Brelidze, Douglas, Ovrut, 0712.3563

KS CYs: Have generalised above method to toric case by embedding CY X into $\otimes_\alpha \mathbb{P}H^0(J_\alpha)$.

Numerical integration

Point sample $p_i \in X$ distributed according to known measure dA :

$$\int_X \mathrm{dVol}_{\mathrm{CY}}\, f \simeq \frac{1}{N}\sum_{i=1}^{N} \tilde{w}_i \det(g_{\mathrm{CY}}(p_i))\, f(p_i)\,, \qquad \tilde{w}_i = \left.\frac{d^6y}{dA}\right|_{p_i}$$

weights

-> two tasks: 1) Generate point sample and 2) compute metric

Point sampling

CICYs: Use a thm by Shiffman and Zelditch which leads to point sample distributed according to a measure dA based on Fubini-Study forms.

Shiffman, Zelditch, CMP 200 (1999) 661.
Douglas, Karp, Lucik, Reinbacher, hep-th/0612075
Braun, Brelidze, Douglas, Ovrut, 0712.3563

KS CYs: Have generalised above method to toric case by embedding CY X into $\otimes_\alpha \mathbb{P}H^0(J_\alpha)$.

Computing metric

Fully connection feed-forward NN which represents metric.

Computational realisation

Point generator

Generates points on CY with known measure dA

Computational realisation

Point generator

Generates points on CY with known measure dA

Neural network

Computational realisation

Point generator

Generates points on CY with known measure dA

Neural network

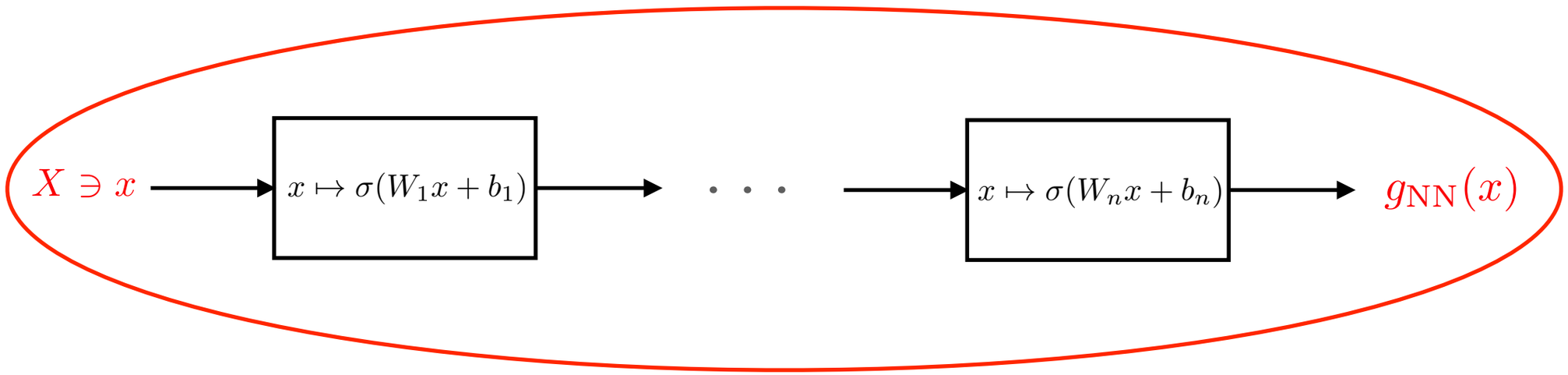

$= g_{\mathrm{NN}}$

Computational realisation

Point generator

Generates points on CY with known measure dA

Neural network

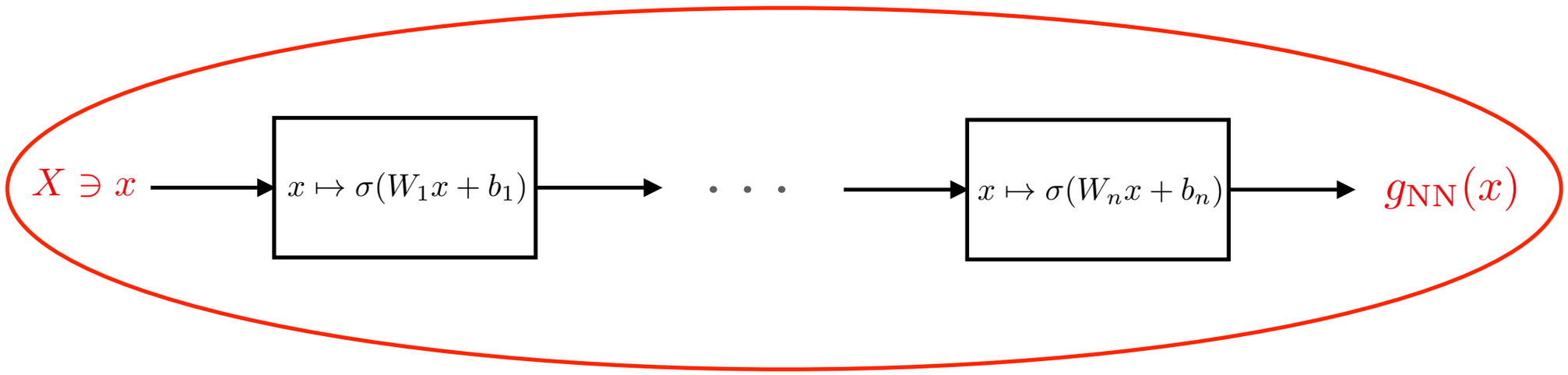

$= g_{\mathrm{NN}}$

Relation between neural network and metric

Name	Ansatz
Free	$g_{\mathrm{pr}} = g_{\mathrm{NN}}$
Additive	$g_{\mathrm{pr}} = g_{\mathrm{FS}} + g_{\mathrm{NN}}$
Multiplicative, element-wise	$g_{\mathrm{pr}} = g_{\mathrm{FS}} + g_{\mathrm{FS}} \odot g_{\mathrm{NN}}$
Multiplicative, matrix	$g_{\mathrm{pr}} = g_{\mathrm{FS}} + g_{\mathrm{FS}} \cdot g_{\mathrm{NN}}$
ϕ-model	$g_{\mathrm{pr}} = g_{\mathrm{FS}} + \partial\bar{\partial}\phi$

Loss function

$$\mathcal{L} = \alpha_1 \mathcal{L}_{\mathrm{MA}} + \alpha_2 \mathcal{L}_{\mathrm{dJ}} + \alpha_3 \mathcal{L}_{\mathrm{transition}} + \alpha_4 \mathcal{L}_{\mathrm{Ricci}} + \alpha_5 \mathcal{L}_{\mathrm{Kclass}}$$

Loss function

$$\mathcal{L} = \alpha_1 \mathcal{L}_{\text{MA}} + \alpha_2 \mathcal{L}_{\text{dJ}} + \alpha_3 \mathcal{L}_{\text{transition}} + \alpha_4 \mathcal{L}_{\text{Ricci}} + \alpha_5 \mathcal{L}_{\text{Kclass}}$$

Monge-Ampere loss: $\mathcal{L}_{\text{MA}} = \left|\left| 1 - \frac{1}{\kappa} \frac{\det g_{\text{pr}}}{\Omega \wedge \bar{\Omega}} \right|\right|_n$

Kahler loss: $\mathcal{L}_{\text{dJ}} = \sum_{ijk} ||\text{Re } c_{ijk}||_n + ||\text{Im } c_{ijk}||_n \qquad c_{ijk} = g_{i\bar{j},k} - g_{k\bar{j},i}$

transition loss: $\mathcal{L}_{\text{transition}} = \frac{1}{d} \sum_{\mathcal{U},\mathcal{V}} \left|\left| g^{\mathcal{V}}_{\text{pr}} - T_{\mathcal{U}\mathcal{V}} \cdot g^{\mathcal{U}}_{\text{pr}} \cdot (T_{\mathcal{U}\mathcal{V}})^\dagger \right|\right|_n$

Ricci loss: $\mathcal{L}_{\text{Ricci}} = ||R||_n = \left|\left| \partial\bar{\partial} \ln \det g_{\text{pr}} \right|\right|_n$

Kahler class loss: $\mathcal{L}_{\text{Kclass}} = \frac{1}{h^{1,1}(X)} \sum_{\alpha=1}^{h^{1,1}(X)} \left|\left| \mu_t(\mathcal{O}_X(e_\alpha)) - \int_X J^2_{\text{pr}} \wedge F_{\text{FS},\alpha} \right|\right|_n$

Loss function

$$\mathcal{L} = \alpha_1 \mathcal{L}_{\text{MA}} + \alpha_2 \mathcal{L}_{\text{dJ}} + \alpha_3 \mathcal{L}_{\text{transition}} + \alpha_4 \mathcal{L}_{\text{Ricci}} + \alpha_5 \mathcal{L}_{\text{Kclass}}$$

Monge-Ampere loss: $\mathcal{L}_{\text{MA}} = \left|\left| 1 - \frac{1}{\kappa} \frac{\det g_{\text{pr}}}{\Omega \wedge \bar{\Omega}} \right|\right|_n$

Kahler loss: $\mathcal{L}_{\text{dJ}} = \sum_{ijk} ||\text{Re } c_{ijk}||_n + ||\text{Im } c_{ijk}||_n \qquad c_{ijk} = g_{i\bar{j},k} - g_{k\bar{j},i}$

transition loss: $\mathcal{L}_{\text{transition}} = \frac{1}{d} \sum_{\mathcal{U},\mathcal{V}} \left|\left| g^{\mathcal{V}}_{\text{pr}} - T_{\mathcal{U}\mathcal{V}} \cdot g^{\mathcal{U}}_{\text{pr}} \cdot (T_{\mathcal{U}\mathcal{V}})^\dagger \right|\right|_n$

Ricci loss: $\mathcal{L}_{\text{Ricci}} = ||R||_n = \left|\left| \partial\bar{\partial} \ln \det g_{\text{pr}} \right|\right|_n$

Kahler class loss: $\mathcal{L}_{\text{Kclass}} = \frac{1}{h^{1,1}(X)} \sum_{\alpha=1}^{h^{1,1}(X)} \left|\left| \mu_t(\mathcal{O}_X(e_\alpha)) - \int_X J^2_{\text{pr}} \wedge F_{\text{FS},\alpha} \right|\right|_n$

fixes Kahler class by matching to the known slopes of line bundles

Loss function

$$\mathcal{L} = \alpha_1 \mathcal{L}_{\text{MA}} + \alpha_2 \mathcal{L}_{\text{dJ}} + \alpha_3 \mathcal{L}_{\text{transition}} + \alpha_4 \mathcal{L}_{\text{Ricci}} + \alpha_5 \mathcal{L}_{\text{Kclass}}$$

Monge-Ampere loss: $\mathcal{L}_{\text{MA}} = \left|\left| 1 - \frac{1}{\kappa} \frac{\det g_{\text{pr}}}{\Omega \wedge \bar{\Omega}} \right|\right|_n$

Kahler loss: $\mathcal{L}_{\text{dJ}} = \sum_{ijk} ||\text{Re } c_{ijk}||_n + ||\text{Im } c_{ijk}||_n \qquad c_{ijk} = g_{i\bar{j},k} - g_{k\bar{j},i}$

transition loss: $\mathcal{L}_{\text{transition}} = \frac{1}{d} \sum_{\mathcal{U},\mathcal{V}} \left|\left| g^{\mathcal{V}}_{\text{pr}} - T_{\mathcal{U}\mathcal{V}} \cdot g^{\mathcal{U}}_{\text{pr}} \cdot (T_{\mathcal{U}\mathcal{V}})^\dagger \right|\right|_n$

Ricci loss: $\mathcal{L}_{\text{Ricci}} = ||R||_n = \left|\left| \partial\bar{\partial} \ln \det g_{\text{pr}} \right|\right|_n$

mini-batches

Kahler class loss: $\mathcal{L}_{\text{Kclass}} = \frac{1}{h^{1,1}(X)} \sum_{\alpha=1}^{h^{1,1}(X)} \left|\left| \mu_t(\mathcal{O}_X(e_\alpha)) - \int_X J^2_{\text{pr}} \wedge F_{\text{FS},\alpha} \right|\right|_n$

fixes Kahler class by matching to the known slopes of line bundles

Loss function

$$\mathcal{L} = \alpha_1 \mathcal{L}_{\rm MA} + \alpha_2 \mathcal{L}_{\rm dJ} + \alpha_3 \mathcal{L}_{\rm transition} + \alpha_4 \mathcal{L}_{\rm Ricci} + \alpha_5 \mathcal{L}_{\rm Kclass}$$

Monge-Ampere loss: $\mathcal{L}_{\rm MA} = \left|\left| 1 - \frac{1}{\kappa} \frac{\det g_{\rm pr}}{\Omega \wedge \bar{\Omega}} \right|\right|_n$

Kahler loss: $\mathcal{L}_{\rm dJ} = \sum_{ijk} ||{\rm Re}\ c_{ijk}||_n + ||{\rm Im}\ c_{ijk}||_n \qquad c_{ijk} = g_{i\bar{j},k} - g_{k\bar{j},i}$

transition loss: $\mathcal{L}_{\rm transition} = \frac{1}{d} \sum_{\mathcal{U},\mathcal{V}} \left|\left| g^{\mathcal{V}}_{\rm pr} - T_{\mathcal{U}\mathcal{V}} \cdot g^{\mathcal{U}}_{\rm pr} \cdot (T_{\mathcal{U}\mathcal{V}})^\dagger \right|\right|_n$

Ricci loss: $\mathcal{L}_{\rm Ricci} = ||R||_n = \left|\left| \partial\bar{\partial} \ln \det g_{\rm pr} \right|\right|_n$

mini-batches

Kahler class loss: $\mathcal{L}_{\rm Kclass} = \frac{1}{h^{1,1}(X)} \sum_{\alpha=1}^{h^{1,1}(X)} \left|\left| \mu_t(\mathcal{O}_X(e_\alpha)) - \int_X J^2_{\rm pr} \wedge F_{{\rm FS},\alpha} \right|\right|_n$

large batches

fixes Kahler class by matching to the known slopes of line bundles

Loss function

$$\mathcal{L} = \alpha_1 \mathcal{L}_{\text{MA}} + \alpha_2 \mathcal{L}_{\text{dJ}} + \alpha_3 \mathcal{L}_{\text{transition}} + \alpha_4 \mathcal{L}_{\text{Ricci}} + \alpha_5 \mathcal{L}_{\text{Kclass}}$$

Monge-Ampere loss: $\mathcal{L}_{\text{MA}} = \left|\left| 1 - \frac{1}{\kappa} \frac{\det g_{\text{pr}}}{\Omega \wedge \bar{\Omega}} \right|\right|_n$

Kahler loss: $\mathcal{L}_{\text{dJ}} = \sum_{ijk} ||\text{Re } c_{ijk}||_n + ||\text{Im } c_{ijk}||_n \qquad c_{ijk} = g_{i\bar{j},k} - g_{k\bar{j},i}$

transition loss: $\mathcal{L}_{\text{transition}} = \frac{1}{d} \sum_{\mathcal{U},\mathcal{V}} \left|\left| g^{\mathcal{V}}_{\text{pr}} - T_{\mathcal{U}\mathcal{V}} \cdot g^{\mathcal{U}}_{\text{pr}} \cdot (T_{\mathcal{U}\mathcal{V}})^\dagger \right|\right|_n$

Ricci loss: $\mathcal{L}_{\text{Ricci}} = ||R||_n = \left|\left| \partial\bar{\partial} \ln \det g_{\text{pr}} \right|\right|_n$

mini-batches

Kahler class loss: $\mathcal{L}_{\text{Kclass}} = \frac{1}{h^{1,1}(X)} \sum_{\alpha=1}^{h^{1,1}(X)} \left|\left| \mu_t(\mathcal{O}_X(e_\alpha)) - \int_X J^2_{\text{pr}} \wedge F_{\text{FS},\alpha} \right|\right|_n$

large batches

fixes Kahler class by matching to the known slopes of line bundles

Error measures

$$\sigma = \frac{1}{\text{Vol}_{\text{CY}}} \int_X \left| 1 - \kappa \frac{\Omega \wedge \overline{\Omega}}{(J_{\text{pr}})^n} \right| \qquad \mathcal{R} = \frac{1}{\text{Vol}_{\text{CY}}} \int_X |R_{\text{pr}}|$$

Results

Fermat quintic (benchmark)

(3 hidden layer, width 64, GELU activation, 200000 points, Adam optimiser)

Results

Fermat quintic (benchmark)

(3 hidden layer, width 64, GELU activation, 200000 points, Adam optimiser)

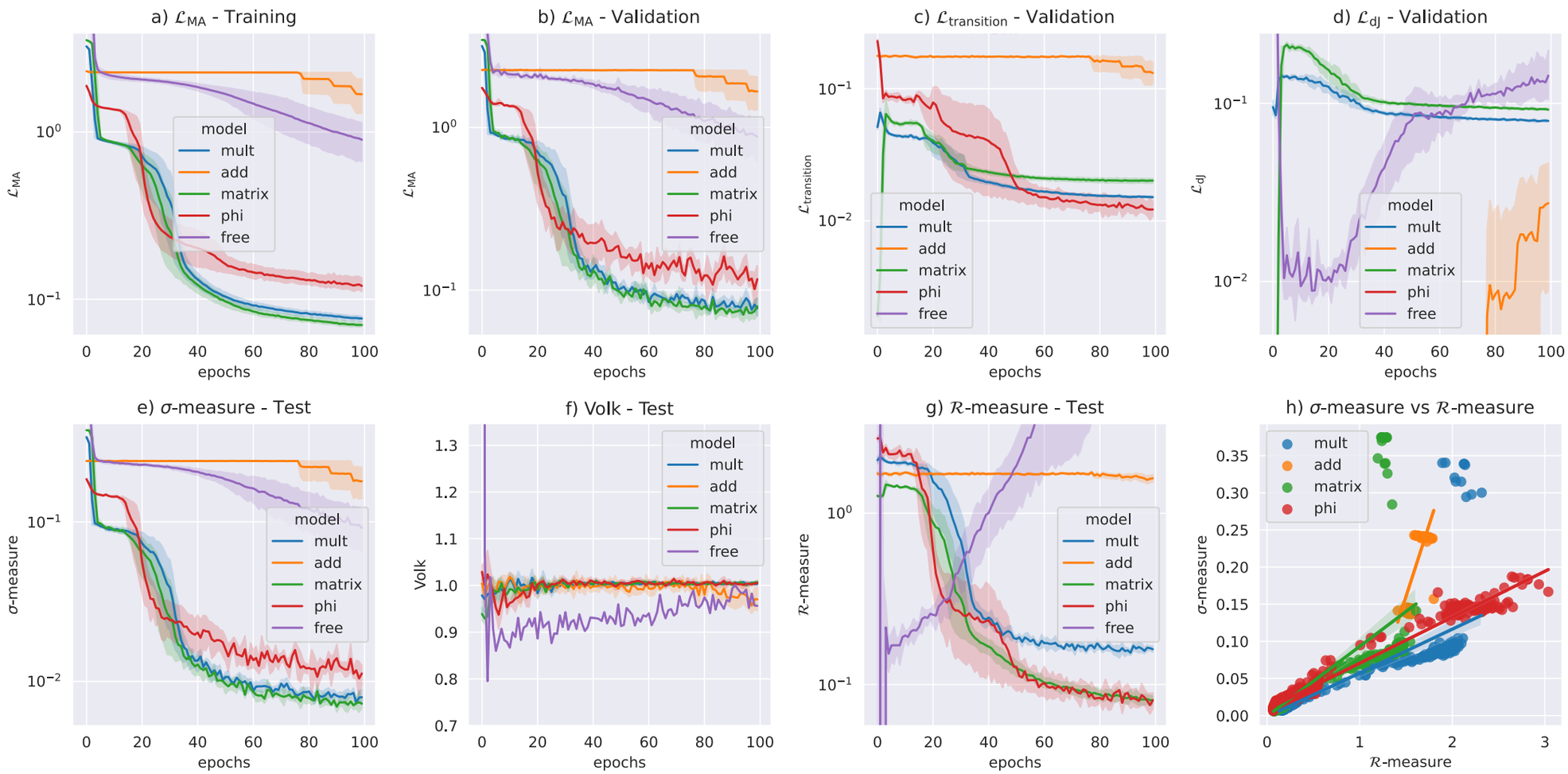

Figure 1: Fermat Quintic experiments: a) Monge-Ampère loss on training data; b)+c)+d) Monge-Ampère, transition and Kähler loss on validation data; e) σ-measure f) volume and g) $\mathcal{R}$-measure on test data; h) the linear relationship between improvement in σ-measure and $\mathcal{R}$-measure. The plots show the averaged performance of five separate experiments for each model, including 95% confidence intervals as light-hue bands around each curve.

Results

Fermat quintic (benchmark)

(3 hidden layer, width 64, GELU activation, 200000 points, Adam optimiser)

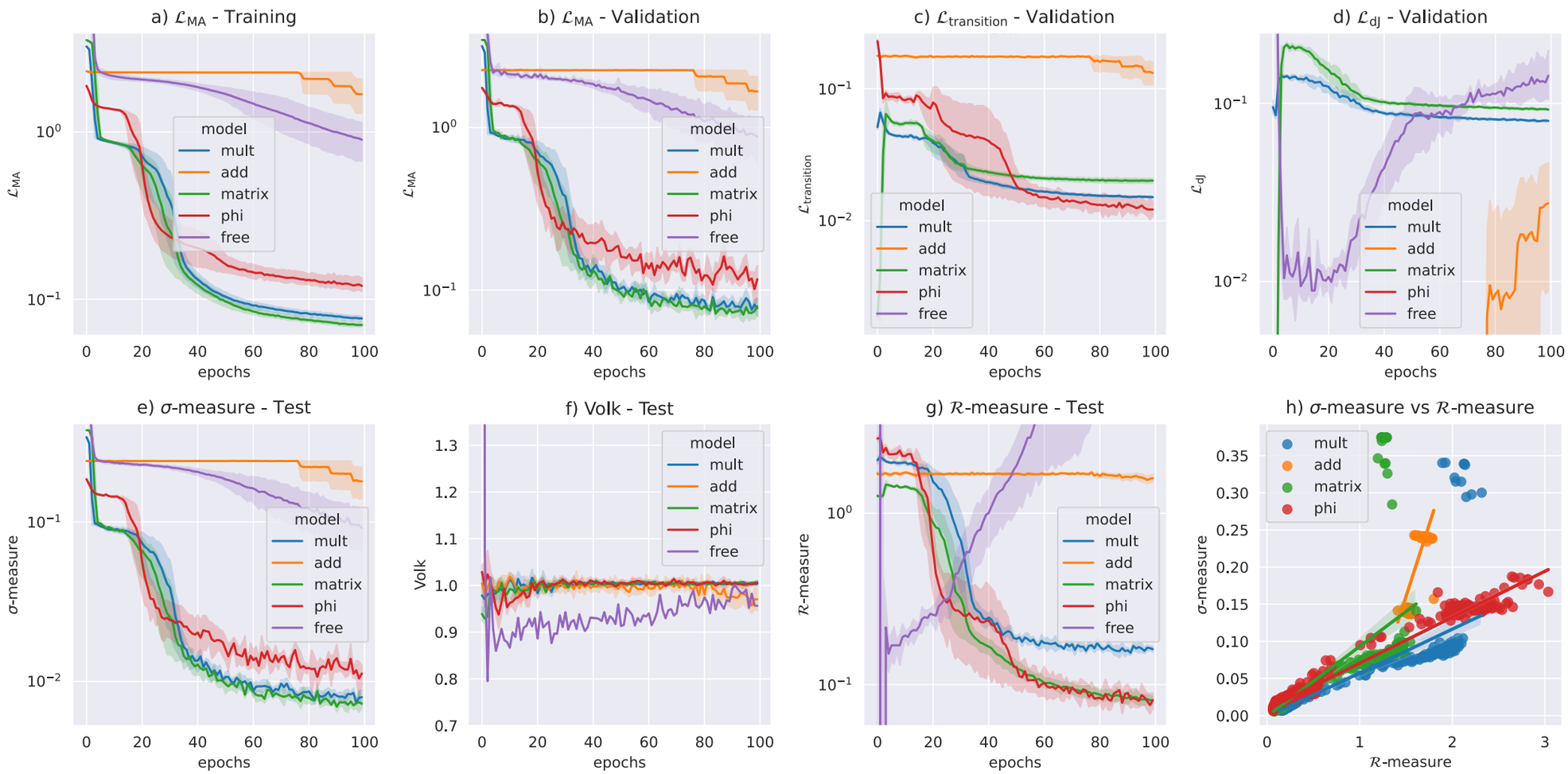

Figure 1: Fermat Quintic experiments: a) Monge-Ampère loss on training data; b)+c)+d) Monge-Ampère, transition and Kähler loss on validation data; e) σ-measure f) volume and g) $\mathcal{R}$-measure on test data; h) the linear relationship between improvement in σ-measure and $\mathcal{R}$-measure. The plots show the averaged performance of five separate experiments for each model, including 95% confidence intervals as light-hue bands around each curve.

- Efficiency comparable to other NN realisations
- ϕ - model most successful

bi-cubic

confgurations: $X \in \left[\begin{array}{c|c} \mathbb{P}^2 & 3 \\ \mathbb{P}^2 & 3 \end{array}\right]^{2,83}_{-162}$ $\begin{array}{l} x_0, x_1, x_2 \\ y_0, y_1, y_2 \end{array}$

bi-cubic

confgurations: $$X \in \left[\begin{array}{c|c} \mathbb{P}^2 & 3 \\ \mathbb{P}^2 & 3 \end{array}\right]^{2,83}_{-162} \qquad \begin{matrix} x_0, x_1, x_2 \\ y_0, y_1, y_2 \end{matrix}$$

defining polynomial (complex structure choice):

$$\begin{aligned} p =& 0.96x_0^3y_0^3 + 0.79x_0^3y_1^3 + 0.49x_0^3y_2^3 + 0.51x_0^3y_0y_1y_2 + 0.05x_1x_0^2y_0y_1^2 + 0.99x_2x_0^2y_0y_2^2 + 0.81x_1x_0^2y_1y_2^2 \\ &+ 0.39x_2x_0^2y_0^2y_1 + 0.54x_1x_0^2y_0^2y_2 + 0.87x_2x_0^2y_1^2y_2 + 0.62x_1x_2x_0y_0^3 + 0.62x_1x_2x_0y_1^3 + 0.62x_1x_2x_0y_2^3 \\ &+ 0.81x_2^2x_0y_0y_1^2 + 0.87x_1^2x_0y_0y_2^2 + 0.54x_2^2x_0y_1y_2^2 + 0.99x_1^2x_0y_0^2y_1 + 0.05x_2^2x_0y_0^2y_2 + 0.39x_1^2x_0y_1^2y_2 \\ &+ 0.87x_1x_2x_0y_0y_1y_2 + 0.49x_1^3y_0^3 + 0.79x_2^3y_0^3 + 0.96x_1^3y_1^3 + 0.49x_2^3y_1^3 + 0.79x_1^3y_2^3 + 0.96x_2^3y_2^3 \\ &+ 0.54x_1^2x_2y_0y_1^2 + 0.39x_1x_2^2y_0y_2^2 + 0.05x_1^2x_2y_1y_2^2 + 0.87x_1x_2^2y_0^2y_1 + 0.81x_1^2x_2y_0^2y_2 + 0.99x_1x_2^2y_1^2y_2 \\ &+ 0.51x_1^3y_0y_1y_2 + 0.51x_2^3y_0y_1y_2 \ , \end{aligned} \tag{5.1}$$

bi-cubic

confgurations: $X \in \left[\begin{array}{c|c} \mathbb{P}^2 & 3 \\ \mathbb{P}^2 & 3 \end{array}\right]^{2,83}_{-162} \qquad \begin{array}{l} x_0, x_1, x_2 \\ y_0, y_1, y_2 \end{array}$

defining polynomial (complex structure choice):

$$\begin{aligned} p =& 0.96x_0^3y_0^3 + 0.79x_0^3y_1^3 + 0.49x_0^3y_2^3 + 0.51x_0^3y_0y_1y_2 + 0.05x_1x_0^2y_0y_1^2 + 0.99x_2x_0^2y_0y_2^2 + 0.81x_1x_0^2y_1y_2^2 \\ &+ 0.39x_2x_0^2y_0^2y_1 + 0.54x_1x_0^2y_0^2y_2 + 0.87x_2x_0^2y_1^2y_2 + 0.62x_1x_2x_0y_0^3 + 0.62x_1x_2x_0y_1^3 + 0.62x_1x_2x_0y_2^3 \\ &+ 0.81x_2^2x_0y_0y_1^2 + 0.87x_1^2x_0y_0y_2^2 + 0.54x_2^2x_0y_1y_2^2 + 0.99x_1^2x_0y_0^2y_1 + 0.05x_2^2x_0y_0^2y_2 + 0.39x_1^2x_0y_1^2y_2 \\ &+ 0.87x_1x_2x_0y_0y_1y_2 + 0.49x_1^3y_0^3 + 0.79x_2^3y_0^3 + 0.96x_1^3y_1^3 + 0.49x_2^3y_1^3 + 0.79x_1^3y_2^3 + 0.96x_2^3y_2^3 \\ &+ 0.54x_1^2x_2y_0y_1^2 + 0.39x_1x_2^2y_0y_2^2 + 0.05x_1^2x_2y_1y_2^2 + 0.87x_1x_2^2y_0^2y_1 + 0.81x_1^2x_2y_0^2y_2 + 0.99x_1x_2^2y_1^2y_2 \\ &+ 0.51x_1^3y_0y_1y_2 + 0.51x_2^3y_0y_1y_2 \ , \end{aligned} \tag{5.1}$$

Choice of Kahler parameters: $J_{\mathrm{FS}} = t^1 J_1 + t^2 J_2$

case	1	2	3	4	5	6	7
$t_{(i)}$	$\begin{pmatrix} 1.414 \\ 1.414 \end{pmatrix}$	$\begin{pmatrix} 0.687 \\ 1.878 \end{pmatrix}$	$\begin{pmatrix} 0.421 \\ 1.955 \end{pmatrix}$	$\begin{pmatrix} 0.299 \\ 1.977 \end{pmatrix}$	$\begin{pmatrix} 0.962 \\ 1.753 \end{pmatrix}$	$\begin{pmatrix} 1.092 \\ 1.676 \end{pmatrix}$	$\begin{pmatrix} 0.853 \\ 1.809 \end{pmatrix}$
$\mathcal{O}_X(k_{(i)})$	$\mathcal{O}_X(1,-1)$	$\mathcal{O}_X(1,-2)$	$\mathcal{O}_X(1,-3)$	$\mathcal{O}_X(1,-4)$	$\mathcal{O}_X(2,-3)$	$\mathcal{O}_X(3,-4)$	$\mathcal{O}_X(3,-5)$

Table 2: Choices $t_{(i)}$, where $i = 1, \ldots, 7$, of the Kähler parameters for the bi-cubic and corresponding slope zero line bundles with line bundle integers $k_{(i)}$.

Training

(3 hidden layer, width 64, GELU activation, 100000 points each, Adam optimiser)

Training

(3 hidden layer, width 64, GELU activation, 100000 points each, Adam optimiser)

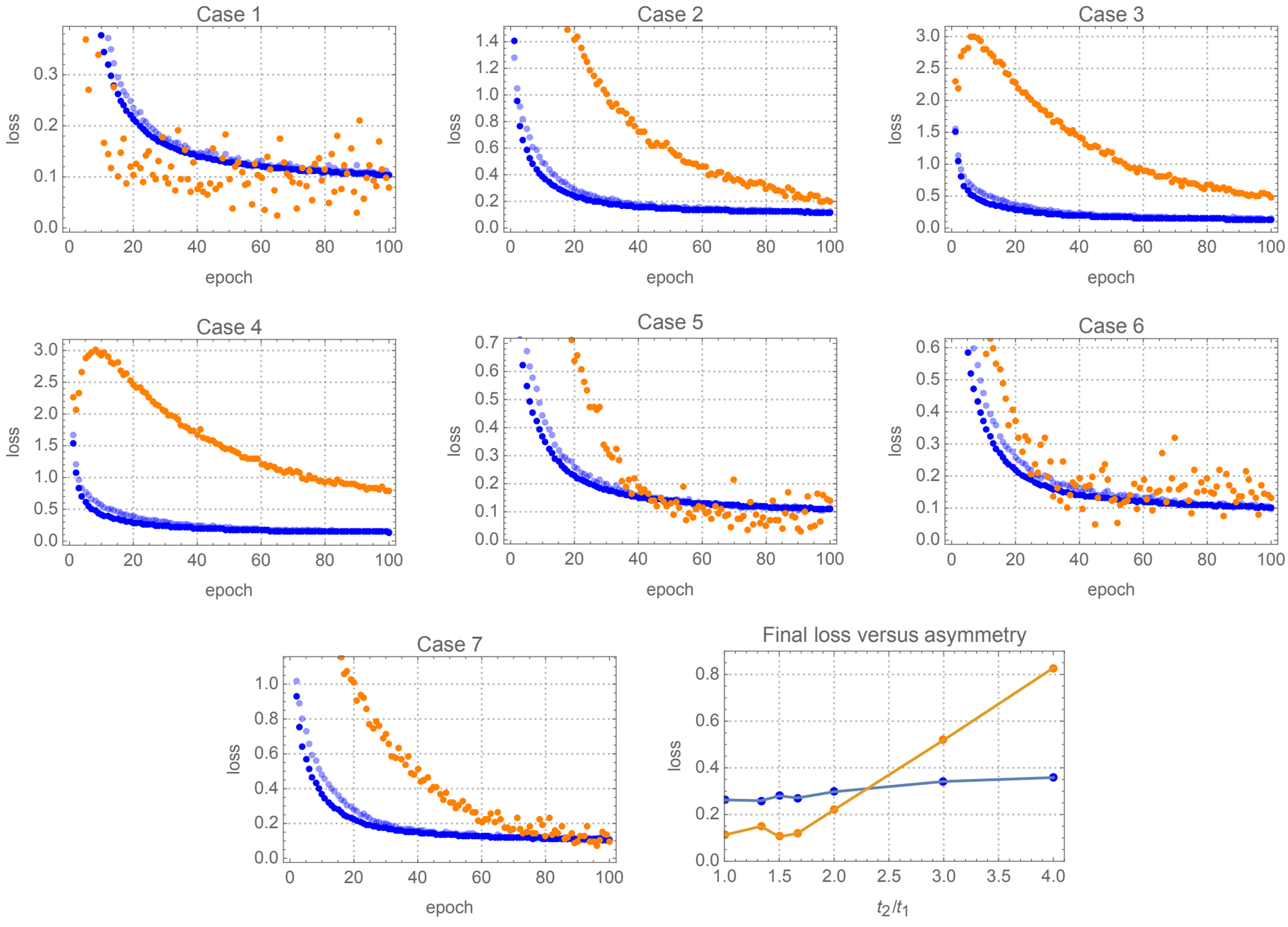

Figure 2: Bi-cubic training curves for the seven choices of Kähler parameters in Table 2. The last plot represents the final loss, obtained by averaging over the last 10 epochs, as a function of t^2/t^1 (orange: $\mathcal{L}_{\text{Kclass}}$, blue: $4 \times \mathcal{L}_{\text{MA}}$, both on training data, light-blue: $4 \times \sigma$ measure on validation data).

Volume check

$$V_{\text{int}} = \frac{1}{6} d_{\alpha\beta\gamma} t^\alpha t^\beta t^\gamma \ , \ V_{\text{FS}} = \frac{1}{N} \sum_{i=1}^{N} \tilde{w}_i \det(g_{\text{FS}}(p_i)) \ , \ V_{\text{CY}} = \frac{1}{N} \sum_{i=1}^{N} \tilde{w}_i \det(g_{\text{CY}}(p_i))$$

case	1	2	3	4	5	6	7
V_{int}	8.49	4.97	2.93	2.02	6.87	7.59	6.16
V_{FS}	8.49	4.50	2.94	2.03	6.91	7.58	6.26
error	$< 1\%$	$< 1\%$	$< 1\%$	$< 1\%$	$< 1\%$	$< 1\%$	$\sim 2\%$
V_{CY}	8.56	5.03	2.96	2.03	6.86	7.58	6.28
error	$< 1\%$	$\sim 1\%$	$< 1\%$	$< 1\%$	$< 1\%$	$< 1\%$	$\sim 2\%$

Table 3: Exact volume from intersection form (row 2), and volume from numerical integration with g_{FS} (row 3) and g_{CY} (row 4), for the seven choices of Kähler parameters in Table 2.

- accurate FS volume -> point sampling sufficient

- accurate CY volume -> Ricci-flat metric accurate, correct Kahler class

slope check

exact slope: $\mu(\mathcal{O}_X(k)) = d_{\alpha\beta\gamma} t^\alpha t^\beta k^\gamma$

$$\mu_{t_{(j)}}(\mathcal{O}_X(k_{(j)})) = \begin{bmatrix} 0.00 & -18.00 & -36.00 & -54.00 & -18.00 & -18.00 & -36.00 \\ 9.16 & 0.00 & -9.16 & -18.33 & 9.16 & 18.33 & 9.16 \\ 10.94 & 5.47 & 0.00 & -5.47 & 16.41 & 27.34 & 21.87 \\ 11.46 & 7.64 & 3.82 & 0.00 & 19.1 & 30.57 & 26.75 \\ 6.45 & -6.45 & -19.34 & -32.24 & 0.00 & 6.45 & -6.45 \\ 4.85 & -9.7 & -24.25 & -38.8 & -4.85 & 0.00 & -14.55 \\ 7.63 & -3.82 & -15.26 & -26.71 & 3.82 & 11.45 & 0.00 \end{bmatrix}$$

slope check

exact slope: $\mu(\mathcal{O}_X(k)) = d_{\alpha\beta\gamma} t^\alpha t^\beta k^\gamma$

$$\mu_{t_{(i)}}(\mathcal{O}_X(k_{(j)})) = \begin{bmatrix} 0.00 & -18.00 & -36.00 & -54.00 & -18.00 & -18.00 & -36.00 \\ 9.16 & 0.00 & -9.16 & -18.33 & 9.16 & 18.33 & 9.16 \\ 10.94 & 5.47 & 0.00 & -5.47 & 16.41 & 27.34 & 21.87 \\ 11.46 & 7.64 & 3.82 & 0.00 & 19.1 & 30.57 & 26.75 \\ 6.45 & -6.45 & -19.34 & -32.24 & 0.00 & 6.45 & -6.45 \\ 4.85 & -9.7 & -24.25 & -38.8 & -4.85 & 0.00 & -14.55 \\ 7.63 & -3.82 & -15.26 & -26.71 & 3.82 & 11.45 & 0.00 \end{bmatrix}$$

FS slope: $\mu(\mathcal{O}_X(k)) = \frac{2}{N\pi} \sum_{i=1}^{N} \tilde{w}_i \det(g_{\mathrm{FS}}(p_i))\, \rho_{\mathrm{FS}}(p_i)$

$$\mu_{t_{(i)}}(\mathcal{O}_X(k_{(j)})) = \begin{bmatrix} 0.11 & -17.84 & -35.78 & -53.73 & -17.73 & -17.62 & -35.57 \\ 9.12 & -0.13 & -9.37 & -18.62 & 8.99 & 18.11 & 8.86 \\ 10.95 & 5.46 & -0.03 & -5.52 & 16.41 & 27.35 & 21.86 \\ 11.47 & 7.65 & 3.82 & -0.01 & 19.12 & 30.6 & 26.77 \\ 6.27 & -6.79 & -19.84 & -32.9 & -0.52 & 5.75 & -7.31 \\ 4.95 & -9.53 & -24.01 & -38.49 & -4.58 & 0.37 & -14.11 \\ 7.34 & -4.43 & -16.19 & -27.95 & 2.91 & 10.25 & -1.51 \end{bmatrix}$$

slope check

exact slope: $\mu(\mathcal{O}_X(k)) = d_{\alpha\beta\gamma} t^\alpha t^\beta k^\gamma$

$$\mu_{t_{(i)}}(\mathcal{O}_X(k_{(j)})) = \begin{bmatrix} 0.00 & -18.00 & -36.00 & -54.00 & -18.00 & -18.00 & -36.00 \\ 9.16 & 0.00 & -9.16 & -18.33 & 9.16 & 18.33 & 9.16 \\ 10.94 & 5.47 & 0.00 & -5.47 & 16.41 & 27.34 & 21.87 \\ 11.46 & 7.64 & 3.82 & 0.00 & 19.1 & 30.57 & 26.75 \\ 6.45 & -6.45 & -19.34 & -32.24 & 0.00 & 6.45 & -6.45 \\ 4.85 & -9.7 & -24.25 & -38.8 & -4.85 & 0.00 & -14.55 \\ 7.63 & -3.82 & -15.26 & -26.71 & 3.82 & 11.45 & 0.00 \end{bmatrix}$$

FS slope: $\mu(\mathcal{O}_X(k)) = \frac{2}{N\pi} \sum_{i=1}^{N} \tilde{w}_i \det(g_{\mathrm{FS}}(p_i))\, \rho_{\mathrm{FS}}(p_i)$

$$\mu_{t_{(i)}}(\mathcal{O}_X(k_{(j)})) = \begin{bmatrix} 0.11 & -17.84 & -35.78 & -53.73 & -17.73 & -17.62 & -35.57 \\ 9.12 & -0.13 & -9.37 & -18.62 & 8.99 & 18.11 & 8.86 \\ 10.95 & 5.46 & -0.03 & -5.52 & 16.41 & 27.35 & 21.86 \\ 11.47 & 7.65 & 3.82 & -0.01 & 19.12 & 30.6 & 26.77 \\ 6.27 & -6.79 & -19.84 & -32.9 & -0.52 & 5.75 & -7.31 \\ 4.95 & -9.53 & -24.01 & -38.49 & -4.58 & 0.37 & -14.11 \\ 7.34 & -4.43 & -16.19 & -27.95 & 2.91 & 10.25 & -1.51 \end{bmatrix}$$

CY slope: $\mu(\mathcal{O}_X(k)) = \frac{2}{N\pi} \sum_{i=1}^{N} \tilde{w}_i \det(g_{\mathrm{CY}}(p_i))\, \rho_{\mathrm{CY}}(p_i)$

$$\mu_{t_{(i)}}(\mathcal{O}_X(k_{(j)})) = \begin{bmatrix} 0.03 & -17.97 & -35.98 & -53.98 & -17.95 & -17.92 & -35.92 \\ 8.86 & -0.42 & -9.70 & -18.98 & 8.43 & 17.29 & 8.01 \\ 10.11 & 4.52 & -1.07 & -6.65 & 14.63 & 24.74 & 19.15 \\ 9.96 & 5.96 & 1.97 & -2.02 & 15.92 & 25.87 & 21.88 \\ 6.38 & -6.45 & -19.29 & -32.12 & -0.07 & 6.31 & -6.53 \\ 4.96 & -9.41 & -23.77 & -38.13 & -4.45 & 0.51 & -13.86 \\ 7.53 & -4.12 & -15.76 & -27.4 & 3.41 & 10.93 & -0.71 \end{bmatrix}$$

slope check

exact slope: $\mu(\mathcal{O}_X(k)) = d_{\alpha\beta\gamma} t^\alpha t^\beta k^\gamma$

$$\mu_{t_{(i)}}(\mathcal{O}_X(k_{(j)})) = \begin{bmatrix} 0.00 & -18.00 & -36.00 & -54.00 & -18.00 & -18.00 & -36.00 \\ 9.16 & 0.00 & -9.16 & -18.33 & 9.16 & 18.33 & 9.16 \\ 10.94 & 5.47 & 0.00 & -5.47 & 16.41 & 27.34 & 21.87 \\ 11.46 & 7.64 & 3.82 & 0.00 & 19.1 & 30.57 & 26.75 \\ 6.45 & -6.45 & -19.34 & -32.24 & 0.00 & 6.45 & -6.45 \\ 4.85 & -9.7 & -24.25 & -38.8 & -4.85 & 0.00 & -14.55 \\ 7.63 & -3.82 & -15.26 & -26.71 & 3.82 & 11.45 & 0.00 \end{bmatrix}$$

FS slope: $\mu(\mathcal{O}_X(k)) = \frac{2}{N\pi} \sum_{i=1}^{N} \tilde{w}_i \det(g_{\mathrm{FS}}(p_i))\, \rho_{\mathrm{FS}}(p_i)$

$$\mu_{t_{(i)}}(\mathcal{O}_X(k_{(j)})) = \begin{bmatrix} 0.11 & -17.84 & -35.78 & -53.73 & -17.73 & -17.62 & -35.57 \\ 9.12 & -0.13 & -9.37 & -18.62 & 8.99 & 18.11 & 8.86 \\ 10.95 & 5.46 & -0.03 & -5.52 & 16.41 & 27.35 & 21.86 \\ 11.47 & 7.65 & 3.82 & -0.01 & 19.12 & 30.6 & 26.77 \\ 6.27 & -6.79 & -19.84 & -32.9 & -0.52 & 5.75 & -7.31 \\ 4.95 & -9.53 & -24.01 & -38.49 & -4.58 & 0.37 & -14.11 \\ 7.34 & -4.43 & -16.19 & -27.95 & 2.91 & 10.25 & -1.51 \end{bmatrix}$$

CY slope: $\mu(\mathcal{O}_X(k)) = \frac{2}{N\pi} \sum_{i=1}^{N} \tilde{w}_i \det(g_{\mathrm{CY}}(p_i))\, \rho_{\mathrm{CY}}(p_i)$

$$\mu_{t_{(i)}}(\mathcal{O}_X(k_{(j)})) = \begin{bmatrix} 0.03 & -17.97 & -35.98 & -53.98 & -17.95 & -17.92 & -35.92 \\ 8.86 & -0.42 & -9.70 & -18.98 & 8.43 & 17.29 & 8.01 \\ 10.11 & 4.52 & -1.07 & -6.65 & 14.63 & 24.74 & 19.15 \\ 9.96 & 5.96 & 1.97 & -2.02 & 15.92 & 25.87 & 21.88 \\ 6.38 & -6.45 & -19.29 & -32.12 & -0.07 & 6.31 & -6.53 \\ 4.96 & -9.41 & -23.77 & -38.13 & -4.45 & 0.51 & -13.86 \\ 7.53 & -4.12 & -15.76 & -27.4 & 3.41 & 10.93 & -0.71 \end{bmatrix}$$

-> Further check of point sampling and correct Kahler class

Application: Compute HYM connection on line bundles

Kreuzer-Skarke CY

fan with vertices: $v_0 = \begin{pmatrix} -1 \\ -1 \\ -1 \\ 0 \end{pmatrix}, \quad v_1 = \begin{pmatrix} 0 \\ 0 \\ 0 \\ 1 \end{pmatrix}, \quad v_2 = \begin{pmatrix} 0 \\ 0 \\ 1 \\ 0 \end{pmatrix}, \quad v_3 = \begin{pmatrix} 0 \\ 1 \\ 0 \\ 0 \end{pmatrix}, \quad v_4 = \begin{pmatrix} 2 \\ 0 \\ 0 \\ -1 \end{pmatrix}, \quad v_5 = \begin{pmatrix} 1 \\ 0 \\ 0 \\ 0 \end{pmatrix},$

$$(h^{1,1}(X), h^{2,1}(X)) = (2, 80)$$

Kreuzer-Skarke CY

fan with vertices:

$$v_0 = \begin{pmatrix} -1 \\ -1 \\ -1 \\ 0 \end{pmatrix}, \quad v_1 = \begin{pmatrix} 0 \\ 0 \\ 0 \\ 1 \end{pmatrix}, \quad v_2 = \begin{pmatrix} 0 \\ 0 \\ 1 \\ 0 \end{pmatrix}, \quad v_3 = \begin{pmatrix} 0 \\ 1 \\ 0 \\ 0 \end{pmatrix}, \quad v_4 = \begin{pmatrix} 2 \\ 0 \\ 0 \\ -1 \end{pmatrix}, \quad v_5 = \begin{pmatrix} 1 \\ 0 \\ 0 \\ 0 \end{pmatrix},$$

$$(h^{1,1}(X), h^{2,1}(X)) = (2, 80)$$

training:

(3 hidden layer, width 256, GELU activation, 200000 points, SGD)

Kreuzer-Skarke CY

fan with vertices:

$$v_0 = \begin{pmatrix} -1 \\ -1 \\ -1 \\ 0 \end{pmatrix}, \quad v_1 = \begin{pmatrix} 0 \\ 0 \\ 0 \\ 1 \end{pmatrix}, \quad v_2 = \begin{pmatrix} 0 \\ 0 \\ 1 \\ 0 \end{pmatrix}, \quad v_3 = \begin{pmatrix} 0 \\ 1 \\ 0 \\ 0 \end{pmatrix}, \quad v_4 = \begin{pmatrix} 2 \\ 0 \\ 0 \\ -1 \end{pmatrix}, \quad v_5 = \begin{pmatrix} 1 \\ 0 \\ 0 \\ 0 \end{pmatrix},$$

$$(h^{1,1}(X), h^{2,1}(X)) = (2, 80)$$

training:

(3 hidden layer, width 256, GELU activation, 200000 points, SGD)

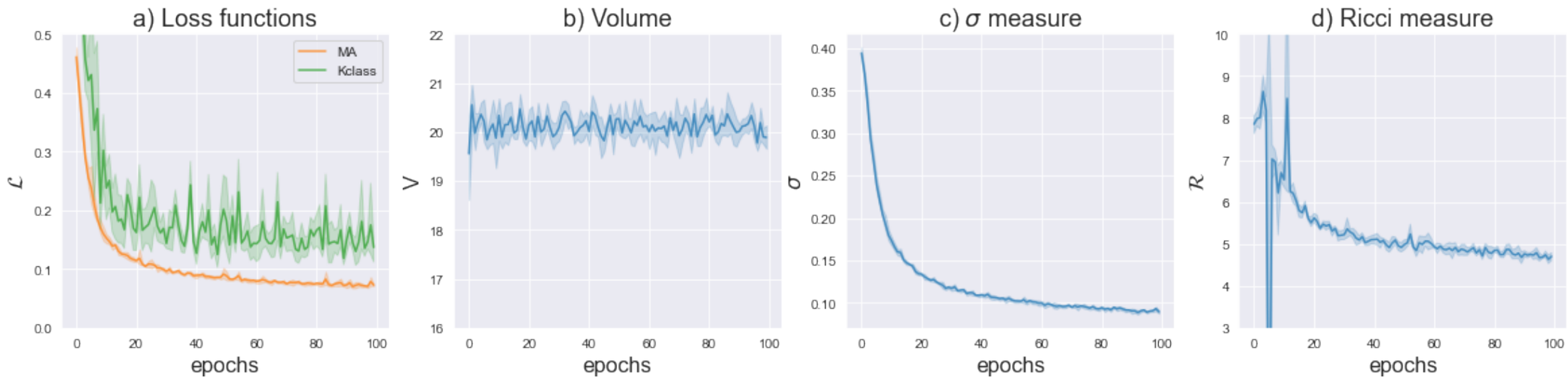

Figure 3: KS CY experiments: a) Monge-Ampère and Kähler class loss on training data; b) volume c) σ measure and d) $\mathcal{R}$ measure on validation data. The plots show the averaged performance of five separate experiments for the ϕ model, including 95% confidence intervals as light-hue bands around each curve.

Conclusion

- We have developed methods to compute Ricci-flat metric for CICYs and KS CYs at given points in moduli space.

- These methods have been realised in package cymetric.

- Experiments for bi-cubic confirm that point sampling and Kahler class fixing works.

- Same confirmed by experiments for KS CY.

Conclusion

- We have developed methods to compute Ricci-flat metric for CICYs and KS CYs at given points in moduli space.

- These methods have been realised in package cymetric.

- Experiments for bi-cubic confirm that point sampling and Kahler class fixing works.

- Same confirmed by experiments for KS CY.

Future directions: More complicated CYs, moduli-dependence of metric, HYM connections on bundles, harmonic forms for matter fields, Yukawa couplings, other special holonomies, G-structure spaces, . . .

Conclusion

- We have developed methods to compute Ricci-flat metric for CICYs and KS CYs at given points in moduli space.

- These methods have been realised in package cymetric.

- Experiments for bi-cubic confirm that point sampling and Kahler class fixing works.

- Same confirmed by experiments for KS CY.

Future directions: More complicated CYs, moduli-dependence of metric, HYM connections on bundles, harmonic forms for matter fields, Yukawa couplings, other special holonomies, G-structure spaces, . . .

Thanks